Supplemental Figure S1. Related to Figures 2E-H.

A

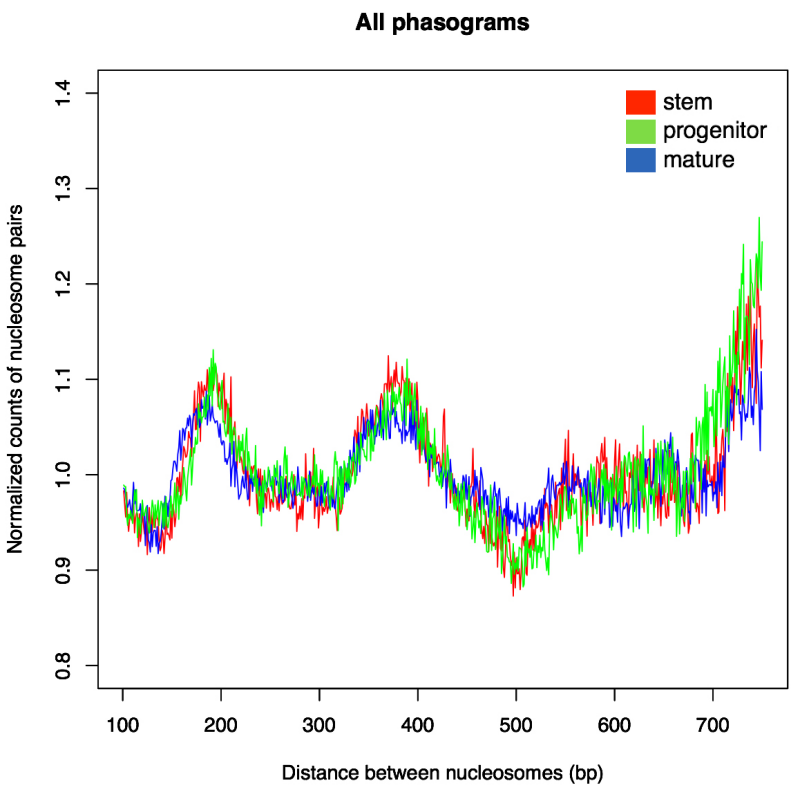

B

	Genomewide (bp)	Expressed genes (bp)	Silent (bp)	Genome fit	Expressed fit	Silent fit
Icam	195.171429	196.3929	196.6786	0.9999658	0.9998896	0.9999014
Ngn	192.4571	191.9643	193.1429	0.999984	0.9996341	0.9999767
Omp	196	192.6786	196.6071	0.9999891	0.9997673	0.99998918

Figure S1. Nucleosome phasing. Related to Figure 2E-H. (A) Phasograms showing normalized counts of the number of nucleosome pairs at each distance apart in 1430 known olfactory receptor genes only. OR genes were obtained from Barbara Trask's laboratory, where overlapping genes were merged. (B) Table summarizing nucleosome periodicity, spacing and phasing data from stem cells (Icam), neuronal progenitor cells (Ngn), and mature olfactory sensory neurons (Omp).

Supplemental Table S1. Related to Figures 2A-D, 3A and 6.

	Stem cells	Progenitor cells	Mature olfactory neurons	HP1β KO
NUCLEUS STATISTICS				
Heterochromatin LAC	0.32 ± 0.01 μm^{-1}	0.31 ± 0.02 μm^{-1}	0.32 ± 0.01 μm^{-1}	0.32 ± 0.01 μm^{-1}
Euchromatin LAC	0.18 ± 0.01 μm^{-1}	0.21 ± 0.02 μm^{-1}	0.23 ± 0.01 μm^{-1}	0.21 ± 0.02 μm^{-1}
Heterochromatin to Euchromatin Ratio	0.33 ± 0.01	0.36 ± 0.02	0.41 ± 0.01	0.23 ± 0.02
Nuclear Volume	123 ± 6 μm^3	114 ± 11 μm^3	105 ± 7 μm^3	209 ± 13 μm^3
Number of Nuclei	25	25	30	25
NUCLEOLUS STATISTICS				
Low LAC	0.23 ± 0.01 μm^{-1}	0.21 ± 0.02 μm^{-1}	0.19 ± 0.01 μm^{-1}	NA
Medium LAC	NA	NA	0.23 ± 0.01 μm^{-1}	NA
High LAC	0.29 ± 0.01 μm^{-1}	0.26 ± 0.02 μm^{-1}	0.27 ± 0.01 μm^{-1}	NA
High LAC Aggregates	0.32 ± 0.01 μm^{-1}	0.29 ± 0.01 μm^{-1}	NA	NA
Number of Nucleoli	10	10	10	NA

Table S1. Table summarizing results of statistical analyses. All analyses were the results of data obtained from multiple different mice and are presented as standard deviation of the mean.

Supplemental Video Legends

Video S1. Related to Figure 1E, Stem cell.
Animation of segmented volume rendered views of the stem cell in Figure 1E color-coded to show heterochromatin (blue), euchromatin (green), mitochondria, bronze; and lipid body, yellow.

Video S2. Related to Figure 1E, Neuronal progenitor.
Animation of segmented volume rendered views of the neuronal progenitor cell in Figure 1E color-coded to show heterochromatin (blue), euchromatin (green), and mitochondria, bronze.

Video S3. Related to Figure 1E, Mature olfactory sensory neuron.
Animation of segmented volume rendered views of the mature olfactory sensory neuron in Figure 1E color-coded to show heterochromatin (blue), euchromatin (green), and mitochondria, bronze.

Video S4. Related to Figure 4A, Stem cell.
Animation slicing through the nucleus of the stem cell in Figure 4A, showing segmented volume rendered views of chromatin color-coded to show heterochromatin (blue) and euchromatin (green).

Video S5. Related to Figure 4B, Neuronal progenitor.
Animation slicing through the nucleus of the neuronal progenitor in Figure 4B, showing segmented volume rendered views of chromatin color-coded to show heterochromatin (blue) and euchromatin (green).

Video S6. Related to Figure 4C, Mature olfactory sensory neuron..
Animation slicing through the nucleus of the mature neuron in Figure 4C, showing segmented volume rendered views of chromatin color-coded to show heterochromatin (blue) and euchromatin (green).

Video S7. Related to Figure 4D, HP1β KO.
Animation slicing through the nucleus of the HP1β KO in Figure 4D, showing segmented volume rendered views of chromatin color-coded to show heterochromatin (blue) and euchromatin (green).

Video S8. Related to Figure 5, Stem cell.
Animation of the heterochromatin skeletonized structure of the stem cell shown in Figure 5. Red denotes a small minimum distance, or thin region, of a branch of the heterochromatic structure; white denotes a large minimum distance, or thick region, of a branch of the heterochromatin.

Video S9. Related to Figure 5, Neuronal progenitor.
Animation of the heterochromatin skeletonized structure of the neuronal progenitor shown in Figure 5. Red denotes a small minimum distance, or thin region, of a branch of the heterochromatic structure; white denotes a large minimum distance, or thick region, of a branch of the heterochromatin.

Video S10. Related to Figure 5, Mature olfactory sensory neuron.
Animation of the heterochromatin skeletonized structure of the mature neuron shown in Figure 5. Red denotes a small minimum distance, or thin region, of a branch of the heterochromatic structure; white denotes a large minimum distance, or thick region, of a branch of the heterochromatin.

Video S11. Related to Figure 5, HP1β KO.
Animation of the heterochromatin skeletonized structure of the HP1β KO shown in Figure 5. Red denotes a small minimum distance, or thin region, of a branch of the heterochromatic structure; white denotes a large minimum distance, or thick region, of a branch of the heterochromatin.

Video S12. Related to Figure 6A and B, Nucleolus.
Animation of the nucleolus shown in Figure 6A,B showing the sequential addition of segmented surface views of the nucleolar zones, green (LAC, 0.19 μm^{-1}), blue (LAC, 0.23 μm^{-1}), and red (LAC, 0.27 μm^{-1}). A thin shell of the heterochromatin masses in contact with the nucleolus is shown in blue.

Supplemental Experimental Procedures

Mice
For mature olfactory sensory neurons we used knock-in OMPiresGFP mice; for the neuronal progenitor cells we used Ngn1-GFP BAC transgenics (both described in (Magklara et al., 2011). The two reporter mice have been backcrossed to C57Bl and are maintained in C57Bl background.

Soft X-ray Tomography Data Collection
Neurons were dissociated using papain dissolved in neurobasal A medium supplemented with HEPES, glutamine, and methylcellulose for 30–45 min, after which the reaction was stopped with addition of albumin. Cells were then washed, filtered, loaded into thin walled (200 nm) glass capillaries (in medium), and rapidly frozen by mechanically plunging, at 2 m/sec, into liquid nitrogen cooled propane. This approach optimizes cryo-immobilization of the nucleus. Projection images were collected at 517 eV using XM-2, the National Center for X-ray Tomography soft X-ray microscope at the Advanced Light Source of Lawrence Berkeley National Laboratory; the microscope was equipped with a resolution defining 50-nm objective lens. During data collection, the cells were maintained in a stream of helium gas that had been cooled to liquid nitrogen temperatures (Le Gros et al., 2005; McDermott et al., 2009). Cooling the specimen allows collection of projection images while mitigating the effects of exposure to radiation. For each dataset, 90-180 projection images were collected sequentially around a rotation axis in 1-2° increments to give a total rotation of 180°. An exposure time of between 150 and 300 ms was used (depending on synchrotron ring current). Projection images were manually aligned using IMOD software by tracking fiducial markers on adjacent images (Kremer et al., 1996) and tomographic reconstructions were calculated using the iterative reconstruction method (Mastronarde, 2005; Stayman and Fessler, 2004). LAC values were determined as described previously (Weiss et al., 2001).

Linear Absorption Coefficient (LAC)
The absorption of X-rays by the specimen adheres to the Beer-Lambert law and is therefore linear, quantitative, and a function of thickness and chemical composition (Beer, 1852 and Lambert, 1760). In a SXT reconstruction of a cell, highly solvated regions appear relatively transparent to X-rays compared with regions that are densely packed with biomolecules. After tomographic reconstruction, cells are segmented by bounding regions that have similar attenuation characteristics [this is quantified for each voxel in the reconstruction and is known as the linear absorption contrast (LAC)]. For example, regions in a cell that are mostly composed of biomolecules, such as a lipid droplet, have very high LAC values compared to organelles that are typically much lower in biomolecule density, such as vacuoles. Once segmented, further analysis are carried out on the internal structure of the organelles, again based on the LAC values. For example, regions of different density inside the nucleus can be delineated and segmented.

Soft X-ray Tomography Data Analysis
The LAC histograms that were generated for each nucleus (as described in Experimental Procedures) were analyzed for nuclei within each cell type – stem cells, neuronal progenitors, and mature olfactory sensory neurons. The statistics obtained for each cell type are shown in Table S1 and representative images shown in Figures 2-4. The mean heterochromatin and mean euchromatin values of all nuclei examined were used to determine the relative degree of crowding in these two chromatin regions, which was about 30%. Histogram measurements and the distance of hetero- and eu-chromatin from the nuclear envelope were calculated using MATLAB scripts written by Dr. Markko Myllys (available at ncxt.lbl.gov…..*to be provided at publication*).

Segmentation of Soft X-ray Tomography Data
Nuclei were segmented using the program Amira (VSG, Visualization Sciences Group, an FEI Company). Using the "paintbrush" tool, the outer edge of the nucleus was 'painted' (manually traced using a Wacom drawing pen tablet, DTU-2231; Wacom Technology Corporation, Portland OR) orthoslice-by-orthoslice. Some portions of the nuclear envelope from several adjacent slices could be segmented using a volumetric interpolation tool. After performing initial paintbrush segmentation by selecting through slices along one axis, the selected components were viewed in an orthogonal axis to confirm the continuity and accuracy of the selected region in 3 dimensions and using a 3-dimensional view of the currently selected voxels. Segmented regions were recorded in a "label field," which assigns a unique identity to each voxel in the volume. Mitochondria were segmented semi-automatically using the "magic wand" tool. First, voxels from the nucleus label field were removed to eliminate voxels with a similar LAC value. Then voxels with LAC

values between 0.31-0.35 μm^{-1} (unpubished data) were captured using the "magic wand" tool. All orthoslices along one axis were inspected to confirm the continuity and accuracy of the selected region, then inspected in orthogonal axes and in 3 dimensions; selected voxels were stored in the mitochondrial label field.

Segmentation and Analysis of Nucleoli
Due to the noted heterogeneity between nucleoli of the different cell types (stem, neuronal progenitor, and mature neuron), which likely reflects their physiological state, the nucleoli of each cell type were segmented independently. Semi-automatic segmentation of nucleolar substructure was done in the program Amira (as described above) using LAC values specific for each nucleolar subregion of that cell type (Table S1). We visually checked and validated the voxels that were automatically selected to assure they encompassed the appropriate subregion. A label field was then recorded for each subregion to obtain the volumes and for visualization as described next.

Visualization of Soft X-ray Tomography Data
Visualization of the segmented label fields was done using either the constrained smoothing option of the "SurfaceView" tool in Amira, with the draw style set to "triangle normal" (Figures 1E, 4, and 6) or the 'Voltex' tool for volume rendered data sets (Figures 4 and 7).

Immuno-DNA FISH
Fresh olfactory epithelia were embedded in OCT (Sakura) and frozen. 6uM cryosections were cut, air-dried 30', and fixed in ice-cold 4% PFA for 5 min. Sections were permeabilized with PBS-.1% Triton (PT), DNA

was fragmented with .1M HCl for 15' at RT, digested with 3 mg/ml RNase A in PT for 1 hr at 37 C,

dehydrated by RT ethanol series and baked $45C for 10'. Sections were denatured at 85 C for 5 min in 2xSSC, 75% formamide (Invitrogen), immediately dehydrated in an ice-cold ethanol series and baked $45C for 10'. rDNA and cDNA probes were applied at 5 ng/ul under 8mm circular coverslips, sealed with rubber cement and incubated O/N 37C. Slides were washed in 2xSSC, 55% formamide, .1%NP-40 3x15' at 42C, rinsed in PT, blocked in TNB (Promega TSA kit), incubated 2 hr RT with anti-dig or anti-biotin conjugated to DyLight fluors (Jackson Immunore- search), washed in PT+8% formamide 3x15' and mounted. For immuno-FISH, DAPI and anti-nucleolin antibody (AbCam, ab22758) were used at 1ug/ul; secondary antibodies were Alexa conjugates from Invitrogen. After applying secondary antibody and washing, slides were post-fixed in 1mM EGS in PT at 37C for 10' and rinsed; FISH was then commenced at the HCl step.

Light Microscopy
Confocal images were collected on a Zeiss LSM700 at 1μm intervals. Images are maximum intensity projections of confocal Z-stacks.

Quantification of DNA FISH
The low LAC regions in volume-rendered SXT data (Figure 7B) from ten nuclei and the foci of cDNA speckles (Figure 7C, D) from 100 nuclei in five serial sections were counted using Amira. Since SXT obtains images from intact cells rather than highly processed FISH cells, and images at 50 nm resolution, we can see smaller foci than can be seen in FISH-labeled nuclei. Therefore when counting the low-LAC regions in SXT we counted small foci found within a 500 nm diameter radius as one speckle for comparison for comparison to approximate the lower resolution data from light microscopy.

Supplemental References

Beer (1852). "Bestimmung der Absorption des rothen Lichts in farbigen Flüssigkeiten" (Determination of the absorption of red light in colored liquids), *Annalen der Physik und Chemie*, vol. 86, pp. 78–88.

Kremer, J.R., Mastronarde, D.N., and McIntosh, J.R. (1996). Computer visualization of three-dimensional image data using IMOD. J Struct Biol *116*, 71-76.

Lambert, J.H. (1760). *Photometria sive de mensura et gradibus luminis, colorum et umbrae* [Photometry, or, On the measure and gradations of light, colors, and shade] (Augsburg ("Augusta Vindelicorum"), Germany: Eberhardt Klett).

Le Gros, M.A., McDermott, G., and Larabell, C.A. (2005). X-ray tomography of whole cells. Curr Opin Struct Biol *15*, 593-600.

Magklara, A., Yen, A., Colquitt, B.M., Clowney, E.J., Allen, W., Markenscoff-Papadimitriou, E., Evans, Z.A., Kheradpour, P., Mountoufaris, G., Carey, C.*, et al.* (2011). An epigenetic signature for monoallelic olfactory receptor expression. Cell *145*, 555-570.

Mastronarde, D.N. (2005). Fiducial Marker and Hybrid Alignment Methods for Single-and Double-Axis Tomography. Electron tomography : methods for three-dimensional visualization of structures in the cell, 163-185.

McDermott, G., Le Gros, M.A., Knoechel, C.G., Uchida, M., and Larabell, C.A. (2009). Soft X-ray tomography and cryogenic light microscopy: the cool combination in cellular imaging. Trends Cell Biol *19*, 587-595.

Stayman, J.W., and Fessler, J.A. (2004). Compensation for nonuniform resolution using penalized-likelihood reconstruction in space-variant imaging systems. IEEE Trans Med Imaging *23*, 269-284.

Weiss, D., Schneider, G., Vogt, S., Guttmann, P., Niemann, B., Rudolph, D., and Schmahl, G. (2001). Tomographic imaging of biological specimens with the cryo transmission X-ray microscope. Nuclear Instruments & Methods in Physics Research Section A-Accelerators Spectrometers Detectors & Associated Equipment *467*, 1308-1311.